AD-A088 228 NAVAL RESEARCH LAB WASHINGTON DC F/G 20/9
PLASMA DIAGNOSTICS USING PHOTON-INDUCED CHARGE TRANSFER.(U)
AUG 80 J F SEELY, R C ELTON
UNCLASSIFIED NRL-MR-4317 NL

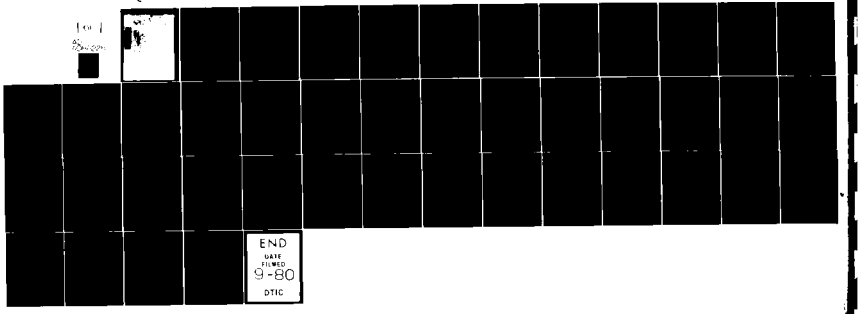

END
DATE FILMED
9-80
DTIC

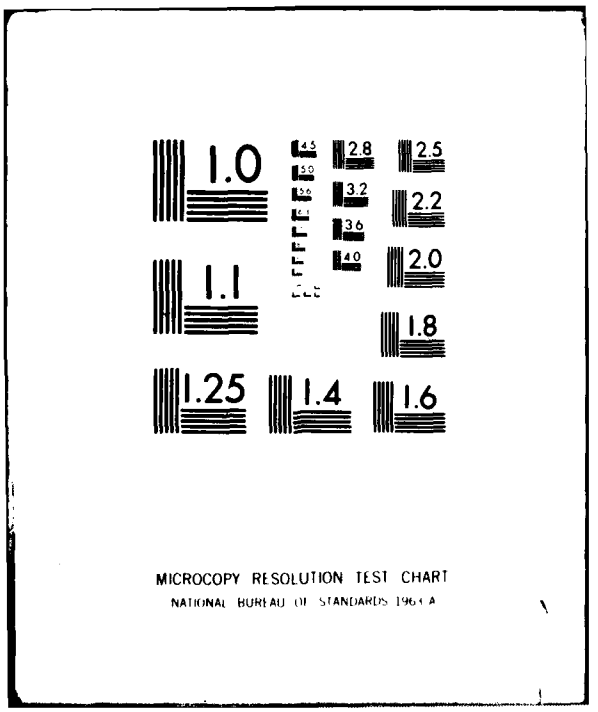
1.0
1.1
1.25
1.4
1.6
1.8
2.0
2.2
2.5
2.8
3.2
3.6
4.0
MICROCOPY RESOLUTION TEST CHART
NATIONAL BUREAU OF STANDARDS 1963 A

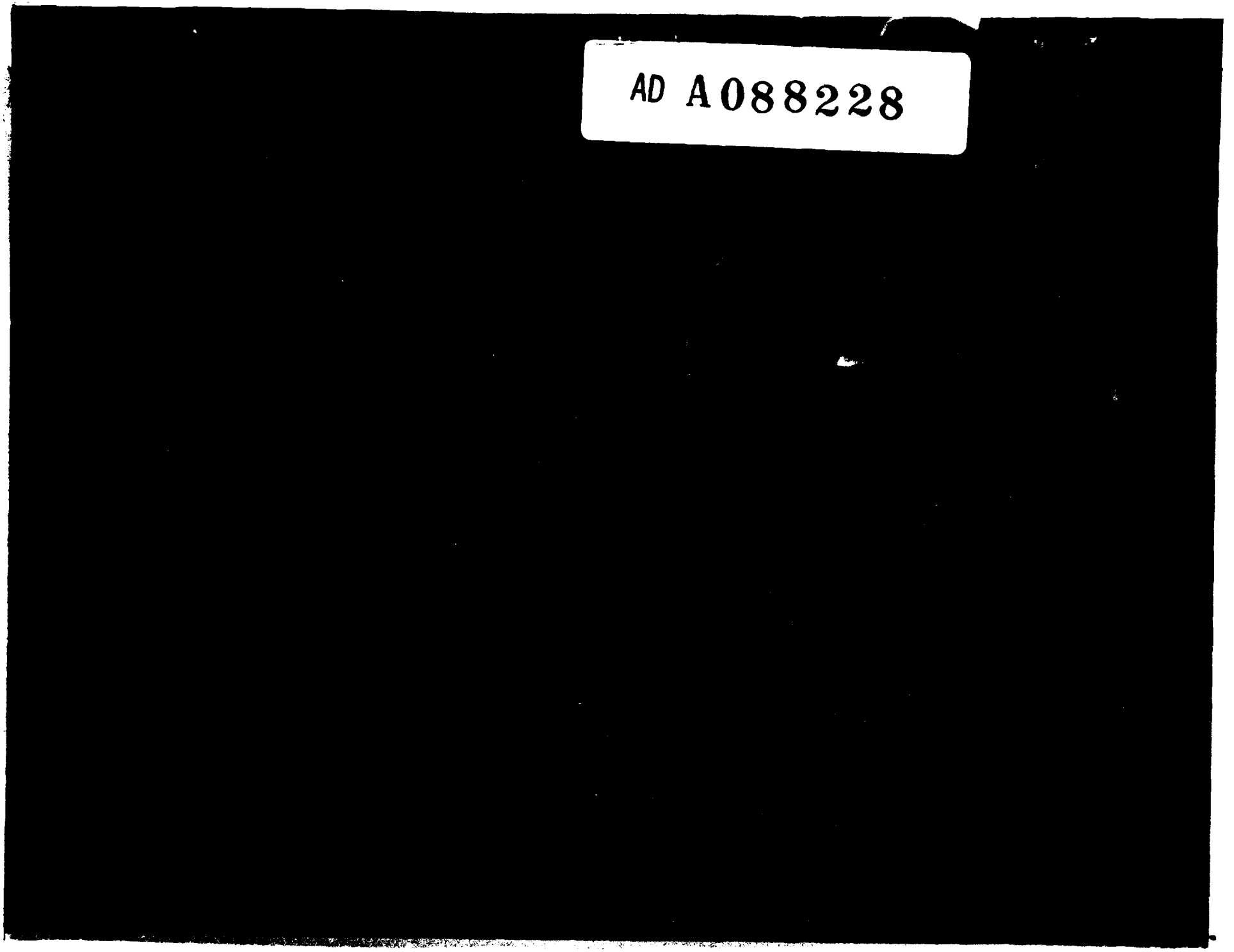

SECURITY CLASSIFICATION OF THIS PAGE *(When Data Entered)*

REPORT DOCUMENTATION PAGE		READ INSTRUCTIONS BEFORE COMPLETING FORM
1. REPORT NUMBER NRL Memorandum report 4317	2. GOVT ACCESSION NO. AD-A088 228	3. RECIPIENT'S CATALOG NUMBER
4. TITLE *(and Subtitle)* PLASMA DIAGNOSTICS USING PHOTON-INDUCED CHARGE TRANSFER		5. TYPE OF REPORT & PERIOD COVERED Interim report on a continuing NRL problem. 6. PERFORMING ORG. REPORT NUMBER
7. AUTHOR(s) J.F. Seely and R.C. Elton		8. CONTRACT OR GRANT NUMBER(s)
9. PERFORMING ORGANIZATION NAME AND ADDRESS Naval Research Laboratory Washington, D.C. 20375		10. PROGRAM ELEMENT, PROJECT, TASK AREA & WORK UNIT NUMBERS 55-1151-0-0; 55-1152-0-0
11. CONTROLLING OFFICE NAME AND ADDRESS		12. REPORT DATE August 18, 1980 13. NUMBER OF PAGES 43
14. MONITORING AGENCY NAME & ADDRESS*(if different from Controlling Office)*		15. SECURITY CLASS. *(of this report)* UNCLASSIFIED 15a. DECLASSIFICATION/DOWNGRADING SCHEDULE

16. DISTRIBUTION STATEMENT *(of this Report)*

Approved for public release; distribution unlimited.

17. DISTRIBUTION STATEMENT *(of the abstract entered in Block 20, if different from Report)*

18. SUPPLEMENTARY NOTES

19. KEY WORDS *(Continue on reverse side if necessary and identify by block number)*

Plasma diagnostics
Charge transfer
Resonance fluorescence

20. ABSTRACT *(Continue on reverse side if necessary and identify by block number)*

A method is described whereby a partner in a binary charge transfer process is photon-excited to a state in which the process can proceed at a greatly enhanced rate. The excited state may be real ("resonance-enhancement") or virtual. With the former, radiative decay fluorescent emission indicates directly the initial state density. Similarly, excited product decay indicates the reaction rate. With known cross sections, this can yield the density of the other reactant under conditions localized in both space and time by the inducing laser pulse. Numerous examples directly applicable to fusion devices are indicated.

DD FORM 1 JAN 73 1473 EDITION OF 1 NOV 65 IS OBSOLETE
S/N 0102-LF-014-6601

SECURITY CLASSIFICATION OF THIS PAGE *(When Data Entered)*

CONTENTS

PLASMA DIAGNOSTICS USING PHOTON-INDUCED CHARGE TRANSFER*

I. INTRODUCTION

Charge transfer is an important atomic process for high temperature plasmas. The cross section is high, particularly near resonance, so that the effect is significant at low densities. Besides representing an additional process that can affect equilibrium and can lead to enhanced radiative energy dissipation, it is important for beam neutralization (as well as reionization) and for particle-beam diagnostics.

The charge transfer process can be represented as

$$D + R^{n+} \rightarrow D^{+} + \left[R^{(n-1)+}\right]^{*} + \Delta E, \qquad (1)$$

where D is the donor atom and R is the receptor or receiver ion which is in an excited (*) state following the reaction. When the energy defect ΔE is large or negative by an amount exceeding the relative motion of the reacting particles, the cross section is low in a nonresonance situation. It has been shown,[1,2] however, that such a nonresonance cross section can be enhanced or "switched" to a value comparable to the resonance value with photons of energy $\simeq \Delta E$; this is called "photon-induced charge transfer". In the general case, the photon may be thought of as exciting

Manuscript submitted July 8, 1980

*Supported in part by the U. S. Department of Energy under agreement EX-76-A-34-1010.

an intermediate virtual state of binding energy satisfying the resonance reaction condition. An intense focused laser beam can shift the binding potential curves until a crossing occurs in the quasi-molecule formed during a collision. As such, this requires a high intensity, and has so far been observed in only one experiment.[3]

Resonance enhancement of photon-induced charge transfer occurs when a real intermediate resonance state is present in the donor atom. Charge transfer can then occur during the lifetime of the excited state, and the cross section approaches that of normal resonance charge transfer for more modest intensities. This has recently been demonstrated[4] for sodium donor atoms excited from 3s to 3p (on the Na-D lines) and receptor ions of H, D, He, Ne, Ar, and Kr.

When the product particle is populated in an excited state [asterisk in Eq. (1)], the radiative decay emission which ensues becomes an indication of the rate of the reaction. When this rate, C, exceeds that of plasma variations, the steady-state rate equation becomes

$$N_D N_R C = N_{R*} A + N_{R*} S, \tag{2}$$

where N_D, N_R, and N_{R*} are the donor, receptor and product densities, respectively, and where A represents the transition probability for the product decay. The parameter S represents the total rate of alternate decay modes, including ionization and other electron collisional depopulation modes as well as other spontaneous decay branches. The measured absolute line emission results in $N_{R*}A$ directly and, with all A's involved known, the righthand side is determined provided that the collisional rates are small; this means choosing a product state with a large

transition probability. With the reaction rate C and the donor density N_D known from theory or experiments, the desired ion density N_R is then determined, resulting in the density diagnostic sought.

In this report, we suggest the use of photon-induced resonance charge transfer reactions as a heavy-particle density probe in plasmas, with measurements localized in both space and time. As an additional advantage, we point out for the first time that a quasi-molecular satellite spectral line may be observable for at least one reaction (p, H) which is shifted sufficiently from the parent Lyman-α line to permit measurement at a lower density in the presence of background line emission. This is particularly important for non-resonantly-enhanced transitions. Also we point out for the first time that measurement of fluorescence from resonance-excited donor atoms D* provides a direct measurement of the initial state density needed to deduce the unknown initial excited-ion density N_{D*}. This synergism of resonance charge transfer with resonance fluorescence replaces the "weak link" that has existed for charge transfer diagnostics--namely an accurate knowledge of the donor state density--while at the same time utilizing laser fluorescence transitions in the "visible" spectral region rather than in the vacuum-uv. A host of potential reaction combinations are given that involve light atoms found typically in contemporary plasma devices (see Tables 1-7).

II. NON-RESONANCE-ENHANCED PHOTON-INDUCED CHARGE TRANSFER

In this section are considered the two cases of protons and alpha particles incident on hydrogen atoms, as examples of non-resonance-enhanced photon-induced charge transfer reactions of plasma interest.

The cross sections for laser-induced charge transfer into the n=2 states of the product ions are calculated using the theory of Ref. 2.

For a low-Z ion incident on hydrogen, the cross section for transfer of the electron from the hydrogen ground state to an excited state of the ion is small at low collision energies, due to the large energy defect between the initial and final electron states. When the collision occurs in the focus of a laser beam, the photon energy makes up the energy defect and enhances the cross section.[1,2] As shown schematically in Fig. 1, the effect of the photon is to shift the potential energy curve of the initial electron state and cause it to intersect the potential energy curve of the final state. If the coupling between the initial and final states is strong at the separation distance R_c of the curve crossing, then charge transfer occurs with high probability.

The experimental observation of laser-induced charge transfer between Ca^+ and Sr has been reported by Green, et al.[3] Copeland and Tang[2] have calculated cross sections for protons incident on Cs and Na.

A. Cross Section Theory

In this section, we outline the cross section theory of Copeland and Tang; the reader is referred to Ref. 2 for more details. Atomic units are used.

In the semiclassical impact-parameter approximation, the two nuclei move on classical trajectories with impact parameter b. The separation of the nuclear motion from the electronic motion is valid for collision velocity much less than one atomic unit, i.e., 2.2×10^8 cm/sec (25 keV protons, 100 keV α-particles). Since the potential energy curves are

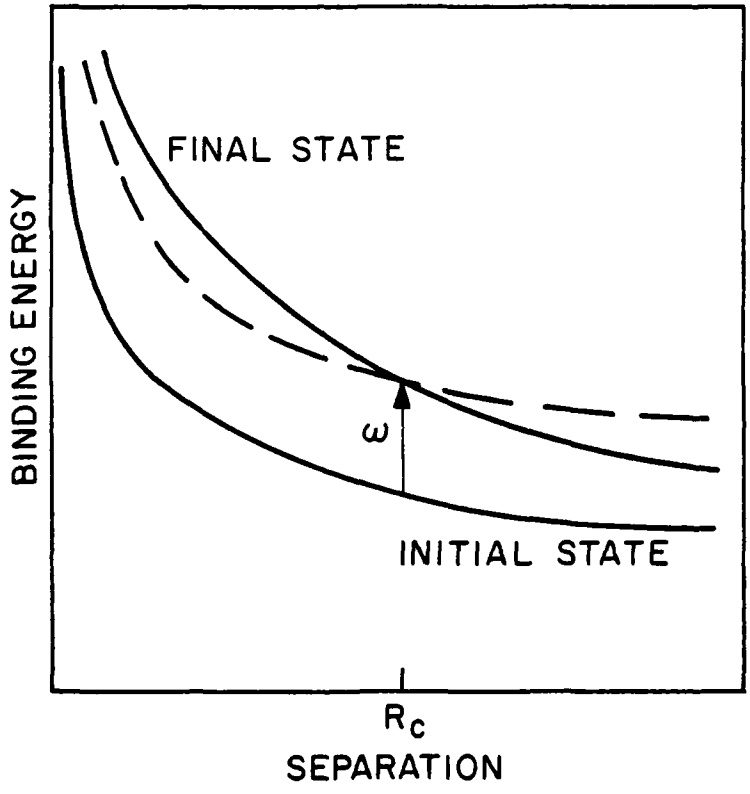

Fig. 1 — Schematic representation of the shift of the initial state by the photon ω and the curve crossing at separation distance R_c.

repulsive at small separation R, the trajectories with small impact parameters are nonlinear. However, the charge transfer reactions considered here are localized at the curve crossing R_c, where the repulsion is negligible for incident energies greater than about 50 eV.

Using first order time-dependent perturbation theory, the transition probability induced by the field $E_o e^{-i\omega t}$ interacting with the dipole moment $d_z(R)$ is

$$P(b,V,E_o) = \alpha^2 \left| \int_b^\infty d_z(R) \cos \Delta(R,b) \frac{b\, dR}{R^2-b^2} \right|^2, \qquad (3)$$

where $$\alpha^2 = E_o^2/V^2 = 7.1 \times 10^{-13} M_{reduced} I\left[W/cm^2\right]/\varepsilon[eV] \qquad (4)$$

and $$\Delta(R,b) = \frac{1}{V}\int_b^R \left[\Delta E(R') - \omega\right] \frac{R'dR'}{\sqrt{R'^2-b^2}} \quad . \qquad (5)$$

In writing Eq. (3), we have assumed that the two states have rotational symmetry about the internuclear axis (σ molecular states) and that $d_z E_o << \omega$ ($I \lesssim 10^{14}$ W/cm^2 for 3500 Å photons and $d_z \simeq 1$ atomic unit).

Due to the cos $\Delta(R,b)$ factor, the integrand of Eq. (3) oscillates rapidly except near the stationary point $d\Delta/dR = 0$. Differentiating Eq. (5), the main contribution to the transition probability occurs when $\Delta E(R) = \omega$. This is the curve crossing point, where the energy difference between the two states ΔE is equal to the photon energy ω. Thus, the charge transfer reaction is localized near the curve crossing point. The transition probability is high if the dipole moment $d_z(R)$ is large in the neighborhood of the crossing point.

The cross section for laser-induced charge transfer is obtained by integrating the transition probability over the impact parameter:

$$\sigma\ (V,\ E_o) = 2\pi \int_o^\infty P(b,\ V,\ E_o)\ b\ db. \tag{6}$$

B. (α,H) Reactions

Consider the reaction

$$He^{+2} + H + \hbar\omega \rightarrow He^{+}\ (n=2) + H^{+} + \Delta E. \tag{7}$$

The exact potential energy curves[5] of the HeH^{+2} quasimolecule are shown in Fig. 2. For the moderate separation distances considered here, the energy difference between the initial and final electron states is approximately equal to the Coulomb potential $\Delta E(R) = 1/R$. In the field of a laser beam, the curves cross at $R_c = 1/\omega$ ($R_c = 7.7$ atomic units for 3500 Å photons). In the region R = 5 to 10 a.u., the strongest radial coupling is between the $2p\sigma$ and $3d\sigma$ states of the HeH^{+2} quasimolecule.[6] The corresponding dipole moment is shown in Fig. 3.

The transition probability calculated from Eq. (3) is shown in Fig. 4 for various collision velocities and pumping wavelengths. The probability peaks when the impact parameter is near the curve crossing point.

The cross section for charge transfer induced by 3500 Å photons is shown in Fig. 5. The experimental cross section[7] for the (no photon) reaction

$$He^{+2} + H\ (1s) \rightarrow He^{+}\ (n=2) + H^{+} + \Delta E \tag{8}$$

is also shown. Laser-induced charge transfer is important at low velocities where the reaction (8) has a negligible cross section, due to large energy defects.

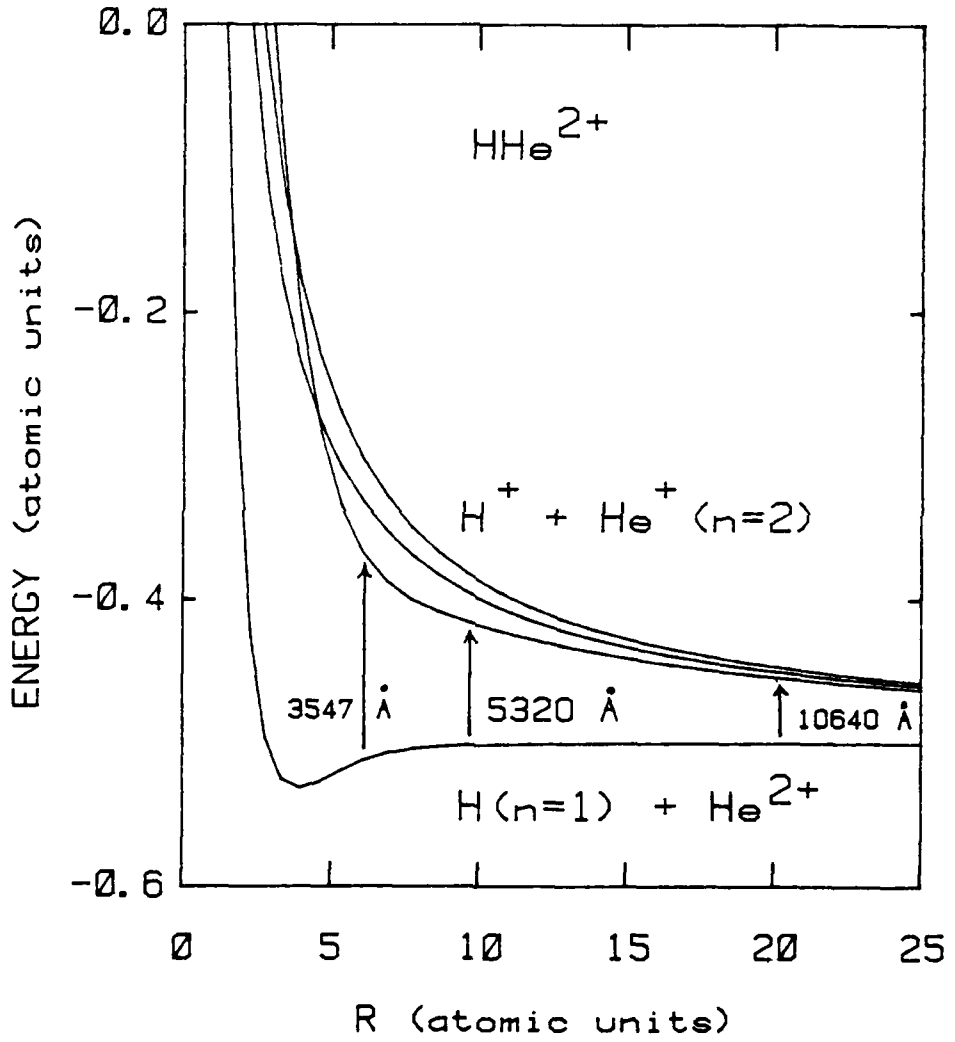

Fig. 2 — The exact potential energy curves (Ref. 5) of the HeH^{+2} quasimolecule. The laser-induced charge transfer is from the $2p\sigma$ state to the $3d\sigma$ state.

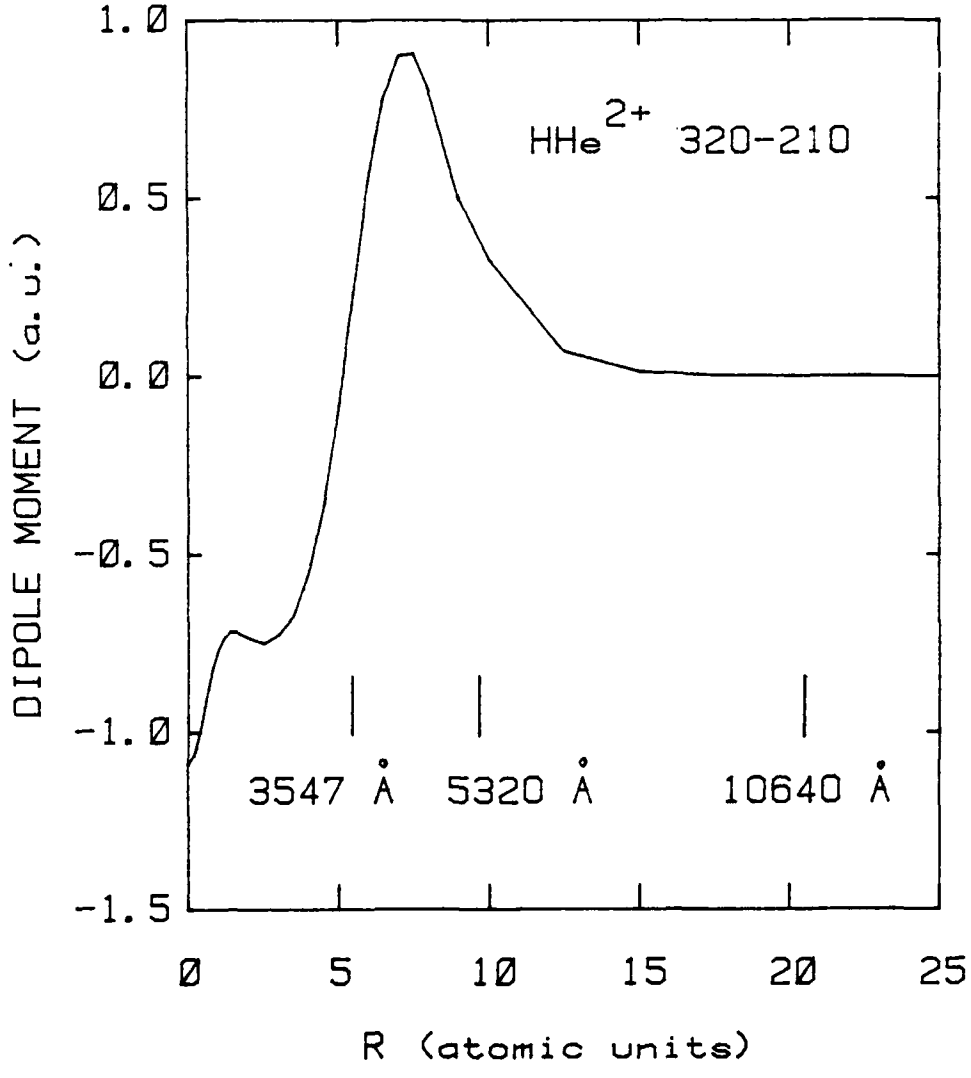

Fig. 3 – The HeH^{+2} dipole moment $-2 < 3d\sigma \left| d/dR \right| 2p\sigma > / \Delta E$ from Ref. 6.

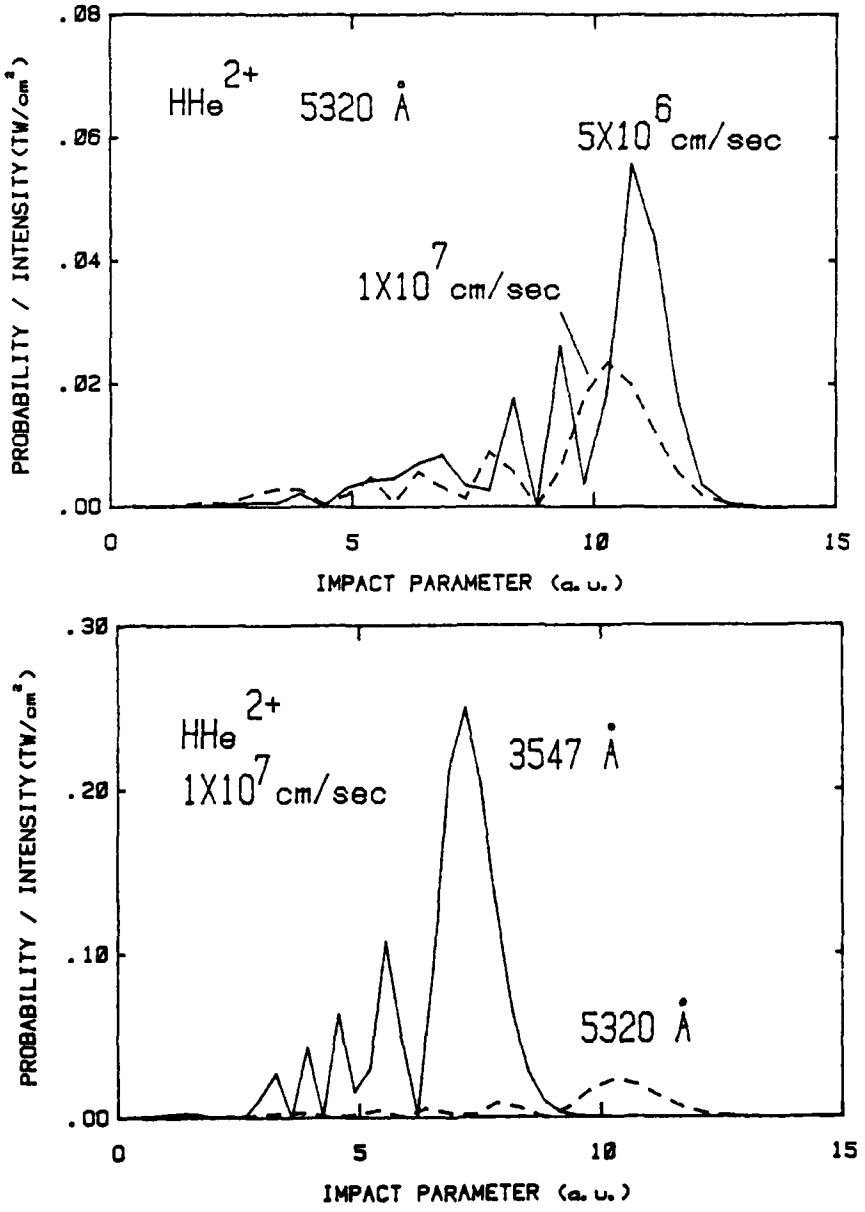

Fig. 4 — Probability for the laser-induced transition HeH^{+2} ($2p\sigma \rightarrow 3d\sigma$).

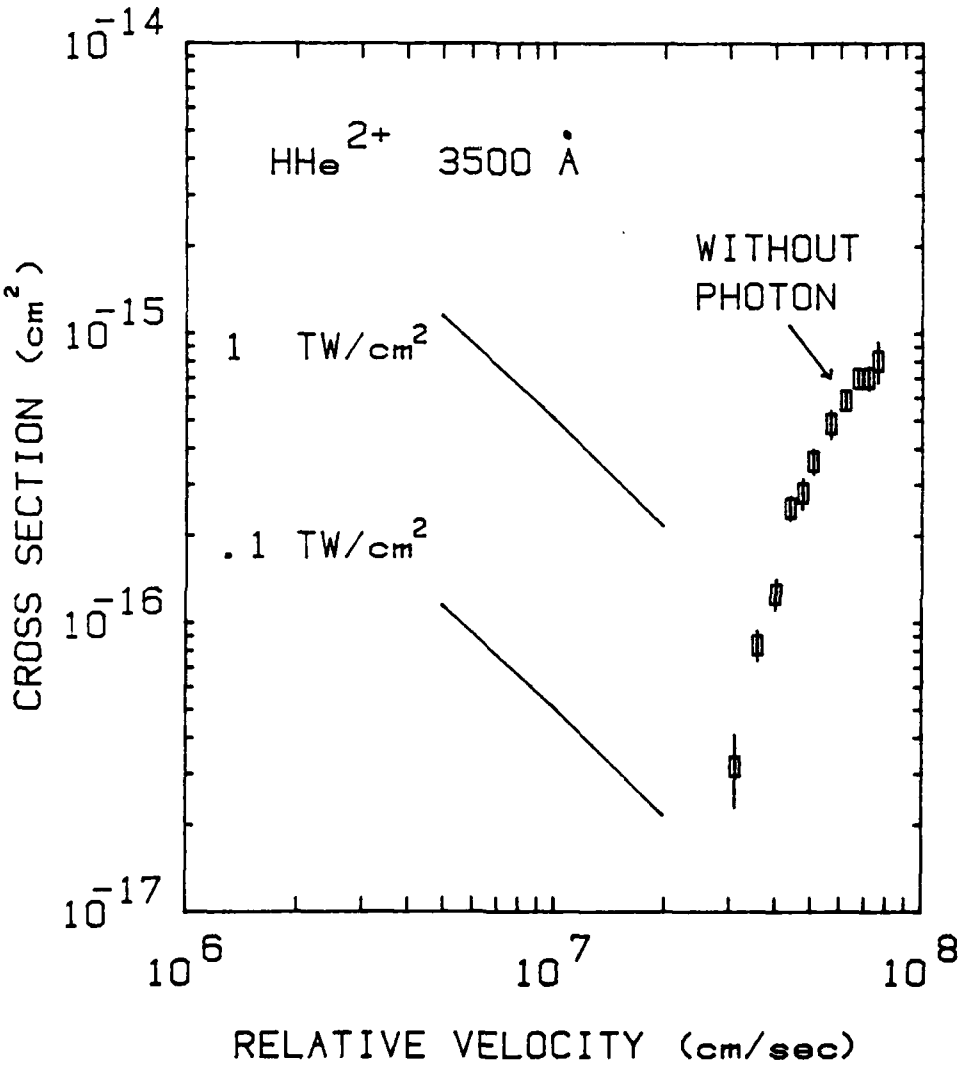

Fig. 5 — Cross section for the laser-induced charge transfer HeH^{+2} ($2p\sigma \rightarrow 3d\sigma$) for 3500 Å pumping radiation. Also shown is the collision-induced cross section from Ref. 7.

The laser-induced charge transfer cross section as a function of pumping wavelength is shown in Fig. 6, where the broad bandwidth is a notable feature. The cross section is largest at wavelengths whose crossing point $R_c = 1/\omega$ are near the peak of the dipole moment curve of Fig. 3.

The cross section for the laser-induced charge transfer reaction

$$Li^{+3} + H(1s) + \hbar\omega \rightarrow Li^{+2}\ (n=3) + H^{+} \qquad (9)$$

should be comparable to that for the α-particle reaction. Here the charge transfer is into the n=3 excited state, and the curve crossing occurs at $R_c = 2/\omega$.

C. (p,H) Reactions

The exact potential energy curves[5] of the H_2^+ quasimolecule are shown in Fig. 7. At small separation R, the 2pσ state is rotationally coupled to the 2pπ state. Collision-induced transitions occur between these two states with high probability, but the cross section is small ($\sim 10^{-17}$ cm^2) due to the small impact parameter.

The field of a laser beam can induce transitions between the radially coupled 2pσ and 2sσ states. As shown in Fig. 8, the dipole moment[8,9] decreases slowly with separation distance R. The transition should occur at as large a separation distance R as possible so that the impact parameter and cross section are also large. Since the energy separation increases with R, this implies a short photon wavelength ($\approx$ 2000 Å at R = 1.5 a.u.).

The cross section for charge transfer induced by 2000 Å photons is shown in Fig. 9. The experimental cross sections[10] for collision-induced

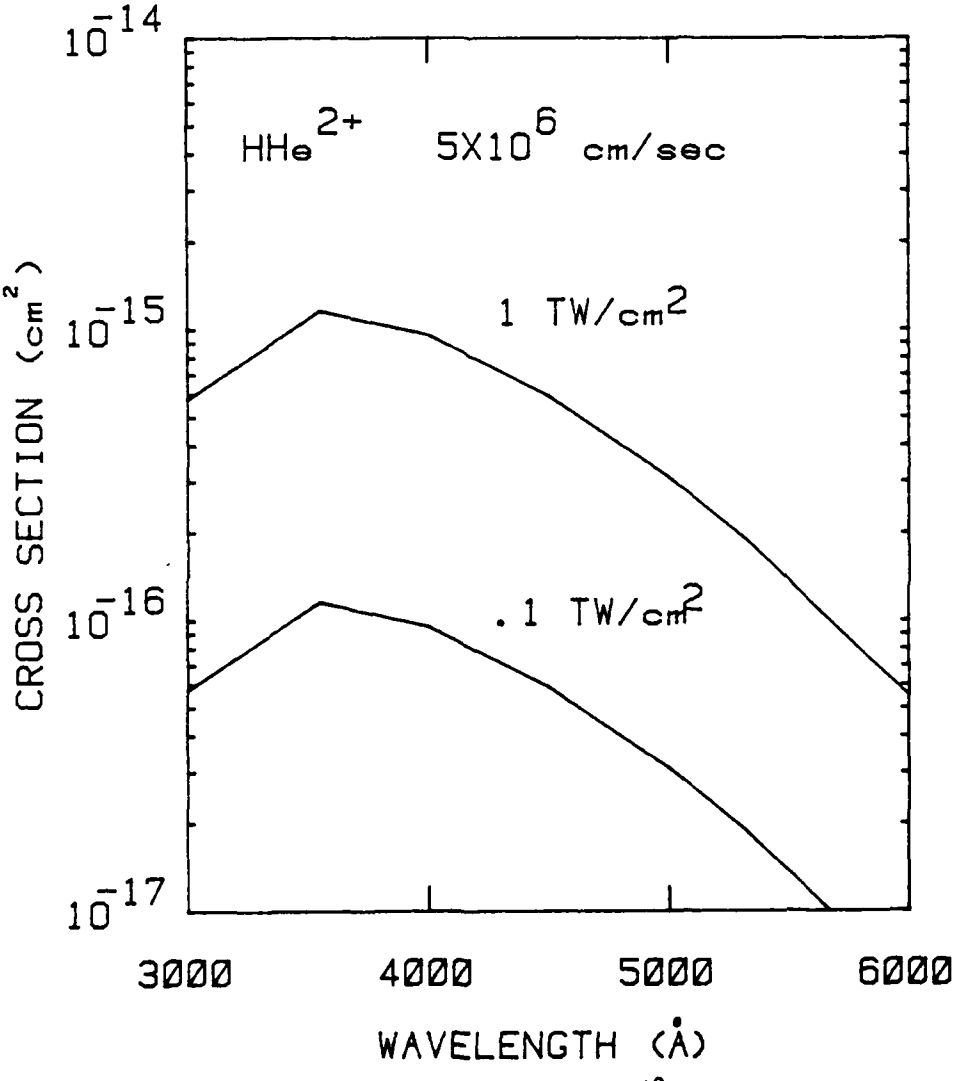

Fig. 6 — Cross section for the laser-induced charge transfer HeH^{+2} ($2p\sigma \rightarrow 3d\sigma$) for a collision velocity of 5×10^6 cm/sec.

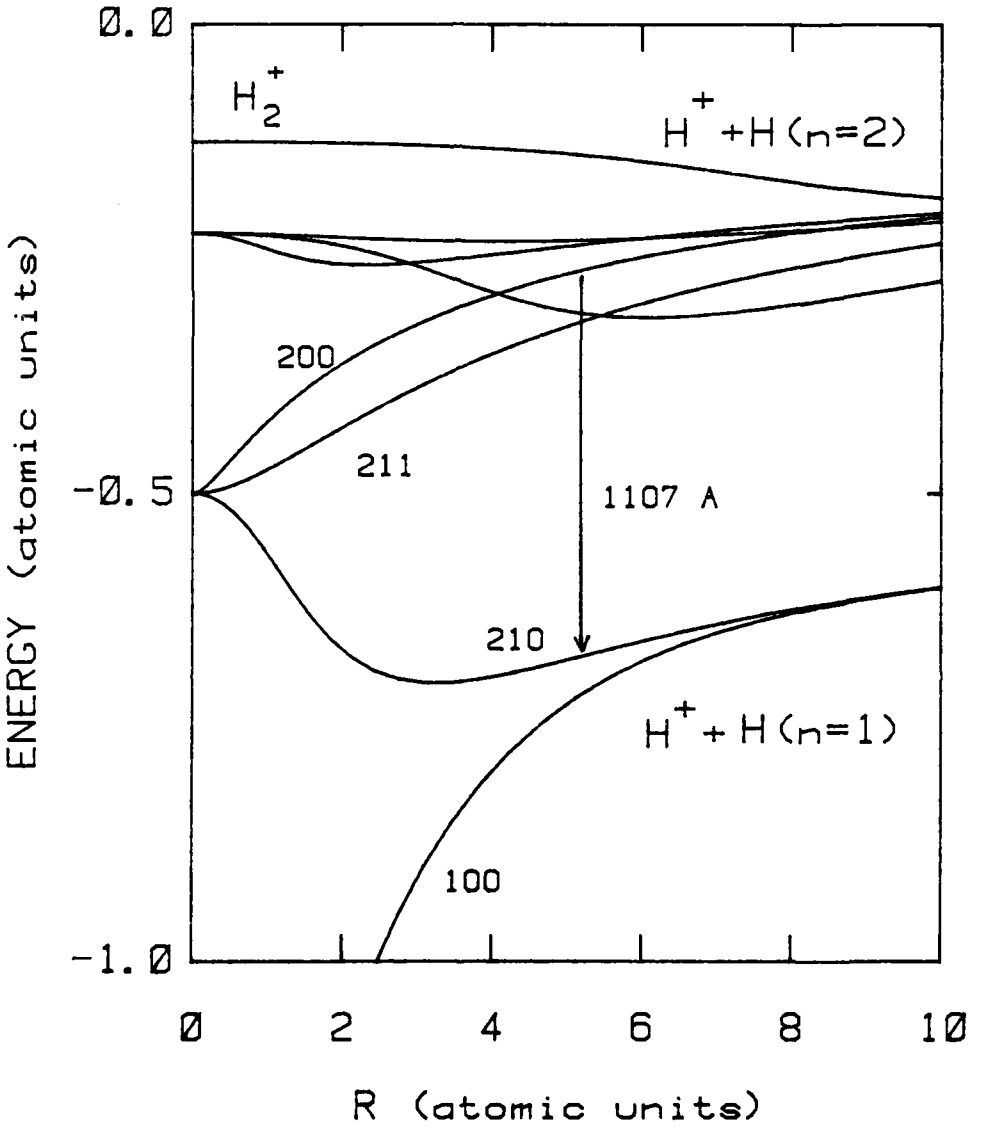

Fig. 7 — The exact potential energy curves (Ref. 5) of the H_2^+ quasimolecule. The laser-induced charge transfer is from the $2p\sigma$ state to the $2s\sigma$ state. The quasimolecule satellite line at 1107 Å is also indicated.

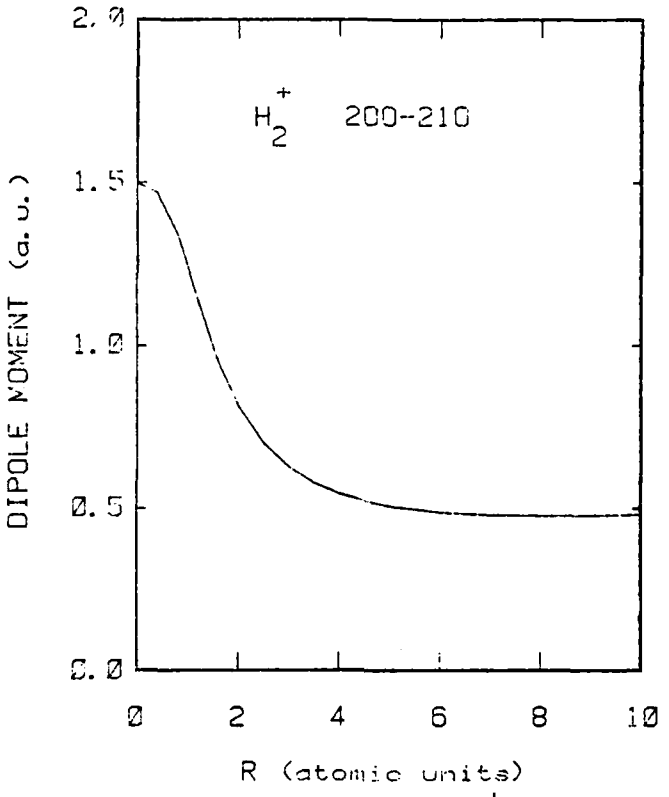

Fig. 8 — The dipole moment (Refs. 8 and 9) for the H_2^+ states $2s\sigma$ and $2p\sigma$.

charge-transfer to the 2s and 2p states of hydrogen are also shown. The laser-induced cross section is large at low collision velocity and high focused laser intensity. The cross section as a function of pumping wavelength is shown in Fig. 10.

D. Localized Density Measurement

The laser-induced charge transfer reactions considered in the previous sections produce n=2 excited states of H and He^+. We now consider the possibility of spectroscopic diagnostics by observing line radiation from these excited states in a plasma. In particular, it is suggested

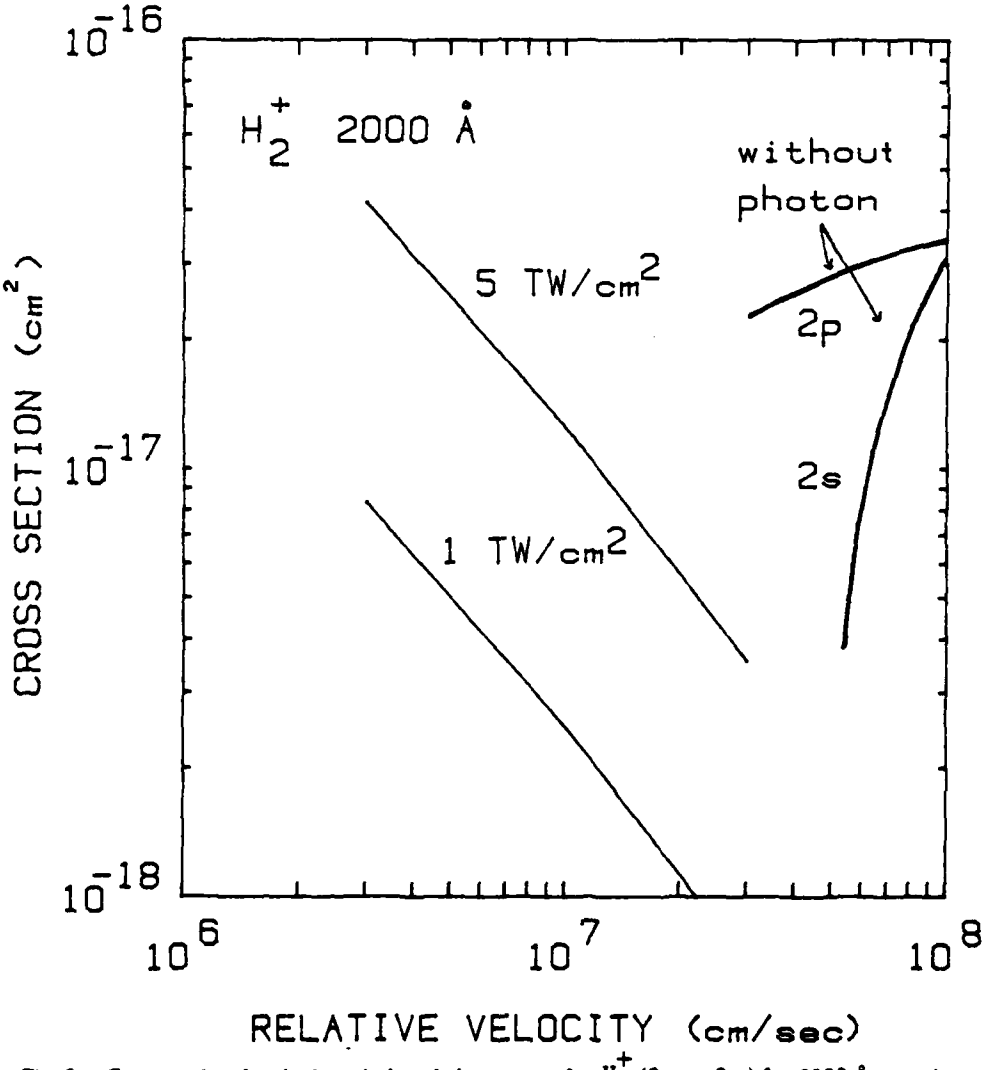

Fig. 9 — Cross section for the laser-induced charge transfer H_2^+ ($2p\sigma \rightarrow 2s\sigma$) for 2000 Å pumping radiation. Also shown are the collision-induced cross sections for transfer to the 2s and 2p states of hydrogen (Ref. 10).

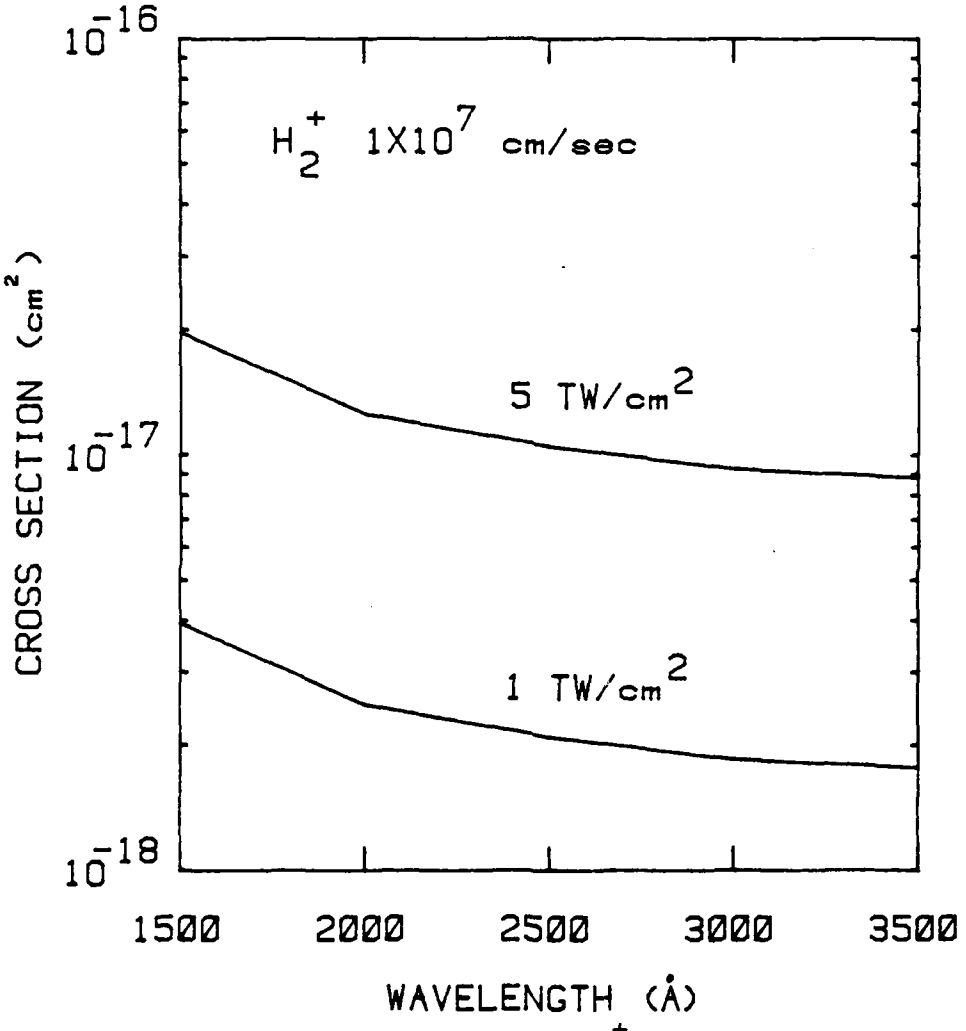

Fig. 10 — Cross section for the laser-induced charge transfer H_2^+ ($2p\sigma \rightarrow 2s\sigma$) for a collision velocity of 1 x 10^7cm/sec.

that a measurement of the (p,H) reaction rate coupled with a knowledge of the proton density (electron density) and the cross section could provide a local measurement of the neutral hydrogen or deuterium density on a time scale determined by the light source. Using a laser, it may even be possible to determine the local temperature by Thomson scattering from the beam directly. A simultaneous (α,H) reaction would then yield the local alpha-particle density, using a known cross section. This example illustrates the extensive potential for this technique.

1. Shifted Line Emission

It may also be possible to observe the quasimolecular satellite line[11] at 1107 Å indicated in Fig. 7. This is a 2 to 1 transition, but it is shifted from the 1216 Å resonance line by the perturbing proton. The absence of a strong resonance line background facilitates the observation of this 1107 Å satellite line, in competition with bremsstrahlung emission.

The hydrogen density required to generate product emission sufficient to overcome a bremsstrahlung background for a Tokamak type plasma is indicated in Figs. 11 and 12 for these reactions.

2. Laser Requirements

As shown in Figs. 6 and 10, the wavelength of the pumping radiation should be about 3500 Å for alphas and somewhat shorter for protons. To achieve appreciable cross sections, the pumping radiation must be focused to a high intensity (greater than 100 GW/cm^2).* This pumping radiation could be produced by frequency multiplying the output of a Nd-glass or ruby laser. Since the laser-induced reactions are not

*Thomson scattering is currently performed on large devices with ruby laser intensities up to 10 GW/cm^2.

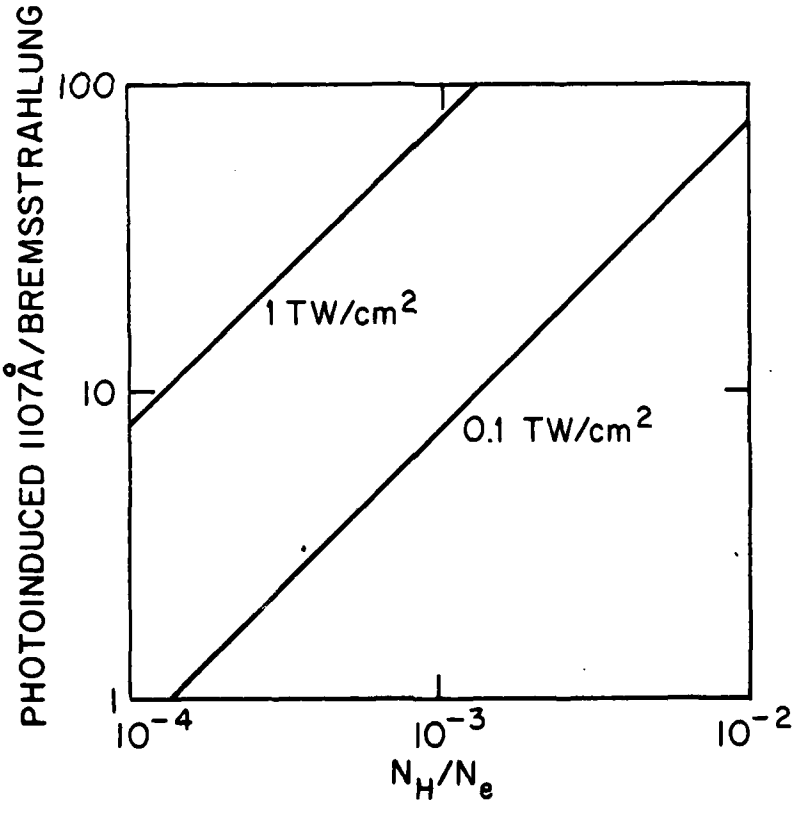

Fig. 11 — The intensity of the photoinduced 1107 Å radiation from the (p, H) reaction divided by the bremsstrahlung intensity (assuming a 1 keV plasma temperature, 1/100 laser focal volume to spectrometer field of view, and 1 Å spectral bandwidth).

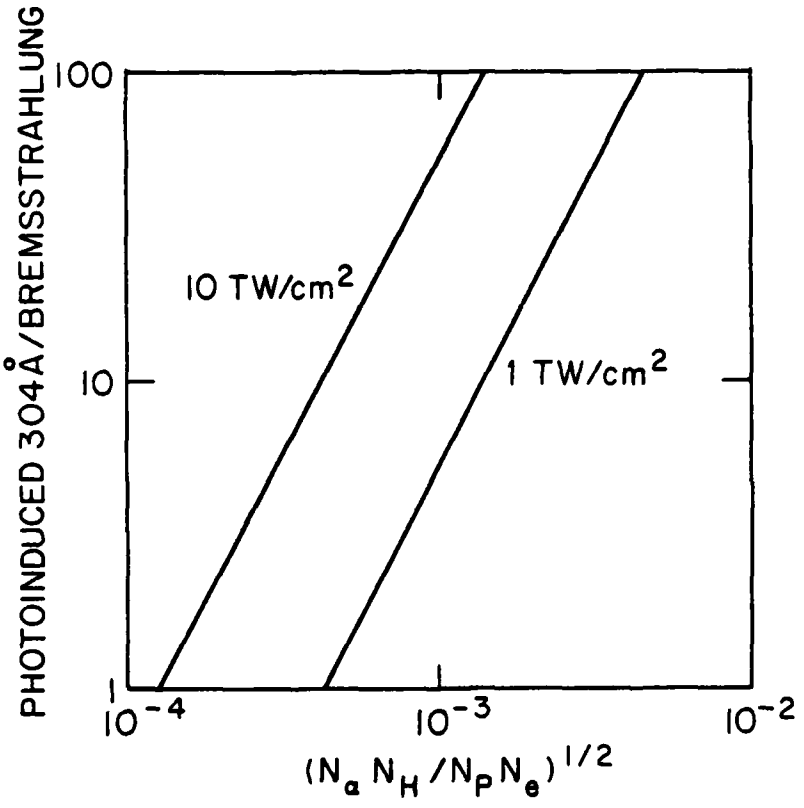

Fig. 12 — The intensity of the photoinduced 304 Å radiation from the (α, H) reaction divided by the bremsstrahlung intensity (assuming a 1 keV plasma temperature, 1/100 laser focal volume to spectrometer field of view, and 1 Å spectral bandwidth).

particularly wavelength selective, it may even be possible to use the broadband output of a flashlamp, focused to high intensity.

3. Applicability for High Energy Alpha Particles

It also has been proposed that reaction (8) be used to measure the density of 3.5 MeV alpha particles in a fusion reactor.[12] An MeV hydrogen beam probes the plasma, and only α-particles with velocities nearly equal to the beam velocity (small relative velocity) have cross sections sufficiently high to interact with the beam. Doppler shifted 304 Å radiation is observed parallel to the hydrogen beam. The presently proposed laser-induced reaction (7) is amenable to the same analysis and could provide additional spatial and temporal resolution.

III. RESONANCE-ENHANCED PHOTON-INDUCED CHARGE TRANSFER

This section describes the resonance-enhancement principle for photon-induced charge transfer, and its promising advantages in reducing the required laser power and particle density. As mentioned in the Introduction, this enhancement in cross section comes about when an allowed excited level in the donor atom is in near-resonance with the reacting ion. For plasma diagnostics, there is again the additional advantage afforded by the resonance fluorescence that results in the donor atom, namely the determination of the initial (excited) state density directly and locally. This effectively removes the major problem that has existed so far in this technique. That is, the donors are usually ground state atoms in high-probability resonance charge transfer reactions, and localized densities for ground states have only been available from broad estimates based on excited-state populations.

Hence, the new idea proposed here is to utilize excited donors in a resonance charge transfer reaction, such that the fluorescent emission from the excited donor atom D* will yield the donor state directly (assuming the transition probability is known).

Population of the excited states might be achieved by electron collisions in some plasmas. However, the population densities may not be sufficient to result in a reaction and a product-feature sufficiently enhanced to distinguish from other plasma radiation. Also, the measurement may not be adequately localized in both space and time. Hence, resonance pumping with, for example, a tunable dye laser appears to offer the best possibility of sufficient excited donor atom production on a highly localized basis, both in space and time. An exception might be lithium and sodium donor atoms where saturation of the low-lying first excited state could yield the ground state density from the measured fluorescence;[13] however, reactions with these ground state donors do not appear promising in the present context.

Laser-pumped resonance fluorescence is also under development as a primary technique for determining the density of (excited) atoms, and usually requires a high power vacuum-ultraviolet laser for many atoms of fusion interest. In the present method, however, a "visible" state-of-the-art tunable dye laser is utilized and ground state densities are determined, using the combined advantages of the resonance fluorescence and charge-transfer processes.

The basis for optimism in achieving resonance charge transfer reactions from laser-pumped excited donors in plasmas is mainly the recent

results of Dutta, et al.,[4] where they succeeded in pumping the 3s-3p transition in neutral sodium using a dye laser tuned to the Na-D wavelength, and transferring preferentially the 3p electrons into the n=2 state of hydrogen formed from proton receptors. The Lyman-α line was enhanced as evidence. The experiments were also repeated with D^+, He^+, Ne^+, Ar^+, and Kr^+ receptors. While normally resonances occurs with exothermic energy defects $\lesssim$ 2000 cm^{-1} (0.25 eV), in the case of Ne^+ they were successful at a reduced rate with a defect of 1.68 eV (13,000 cm^{-1}). While not a fusion-related reaction, such demonstration experiments are useful in establishing feasibility and determining reaction rates, in a well-diagnosed plasma situation.

A. Thermal Charge Transfer Rates

The charge transfer which is involved here falls in the category of a Collision of the Second Kind involving both an ion and an excited atom. There has long been evidence of a large reaction rate when the absolute value of the energy defect is small, and particularly when it is less than ~ 0.25 eV (equiv. to 2000 cm^{-1}) with the defect or "discrepancy" made up by kinetic energy of the partners. Laser pumping by this process is an example. This is also referred to as "asymmetrical" or "accidental" resonance charge transfer, in analogy to symmetrical or exact resonance charge transfer charge transfer involving <u>like</u> partners, one an ion and the other neutral. In the symmetrical case the cross section has been measured[14] to collision energies as low as 20 eV and calculated[15,16] to 0.1 eV. The cross section rises monotonically with decreasing energy and remains fairly constant up to about 10 keV. Asymmetrical cross sections, while in principle different, have

been measured[14] to 25 eV and follow a similar logarithmic $(a-b\log E)^2$ dependence on collision energy until very low energies are reached, where they are expected to decrease for energies approaching zero. This decrease, due to distortion effects[17] which cancel for the symmetrical case, has not been observed; but the energy of maximum cross section E_{max} has been correlated with Massey's abiabatic maximum condition.[18,19]

$$E_{max} = \frac{M}{2}\left[\frac{a\ \Delta E}{h}\right]^2 \qquad (10)$$

in cases where the energy defect ΔE is large $[(H^+,Ne),\ 7.95\ eV]$. Here M is the reduced mass, and $a \simeq 7 \times 10^{-8}$ cm. This strong dependence on energy defect ΔE implies that for lithium projectiles, for example, the cross section remains large for collision energies as low as 1 eV when reactions of energy defect 250 cm^{-1} are involved. What absolute data do exist also indicate that the cross section will be approximately 2×10^{-15} cm^2.

The symmetrical cross section at a fixed velocity (not high) follows closely an inverse power law dependence on ionization energy. Data for the asymmetrical case suggest a similar dependence on the larger ionization potential of the two particles involved, with the magnitude reduced by approximately a factor-of-two.

B. Specific Resonances

In locating suitable resonance, tabulated binding energies between the excited donor electron and the excited final product electron are compared. Exothermic reactions, where the binding energy for the receptor exceeds that for the donor by less than 2000 cm^{-1} (0.25 eV) are considered to be most probable in a resonance. However, endothermic

reactions, where a small energy defect is made up from kinetic energy, are also considered to be possible. Such coincidences are not hard to find among excited states of light atoms, since the binding energies are not all that different far from the core.

First considerations should be limited to neutral donors and singly-ionized receptors, resulting in an ionized donor and a neutral atom; the lack of Coulomb potentials makes the resonance more predictable and the cross section more reliably calculated. Once established, the technique can in principle be expanded to multiple ionization. Potential receptors of interest for fusion then become protons (and deuterons) and ions of helium, carbon, oxygen and silicon, as well as heavier limiter materials. (These represent the ions whose density would be deduced.) This pertains to the plasma core as well as the wall regions.

Concerning the neutral donor atoms, they must be sufficiently plentiful to compete favorably with electron collisional effects on the product atoms. A typical charge transfer cross section is 10^{-15} cm^2, with a rate coefficient σv in the range of 10^{-8} sec^{-1} for thermal ion velocities of 10^7 cm/sec. Electron-collisional rate coefficients are typically in the 10^{-10} sec^{-1} range. Thus, neutral densities in the percent range compared to electrons should suffice. It is possible that such levels of neutral hydrogen or light impurities might exist in the plasma near the wall, but not likely in the hot core; it seems more likely that the neutral donors will have to be added as probe particles. If highly localized at a density in the percent range, the effect both locally and overall on a typical fusion plasma would not be significant.

While no one wants injected particles, there appears to be a resigned acceptance for some neutral beam probing in Tokamaks at present.

Neutral donors of hydrogen, helium, and lithium are fusion-acceptable possibilities. Methods of injection are discussed below. For dye-laser resonance pumping, hydrogen and helium would have to start with n=2 electrons. In the case of hydrogen this means n=2 saturation by Lyman-α emission, presently impractical. Metastable helium n=2 beams are practical and under development at present, so that excited states pumped from the 2^3S and 2^3P states deserve serious consideration at this time. Lithium is particularly promising since the 2s-2p transition can be pumped at 6708 Å, and a host of other excited states can be pumped from these two levels. It may be noted that sodium also has promising aspects similar to lithium, but is less desirable as an additive to a fusion device.

With these considerations in mind, the resonances shown in Tables 1-7 were deduced from published data . Major criteria here were that the reaction be exothermic and that the energy defect be less than 1000 cm^{-1}; only when no possibilities existed and the reaction was considered important did we list possibilities outside of these criteria. Also, strong dipole transitions in the product atom were sought to overcome any competitive decay modes as discussed above; this was also a consideration for the donor atoms in order to effect resonance pumping efficiently without undue plasma perturbation by a focused high power laser beam.

IV. NEUTRAL DONOR INJECTION

A. Beams

Neutral beams do not appear promising for this technique at present. Lithium beams under development for Tokamaks are characteristically 75 keV energy, 10 ma/cm^2 current density, 10^8 cm/sec velocity, and 10^8 cm^{-3} particle density, as needed to penetrate the large plasma with an acceptable level of "loading" of the plasma with lithium during the long pulse involved. Chopping may permit higher densities. Nevertheless, the low donor particle densities available make it unlikely that the product emission from charge transfer reactions could compete with electron collisional excitation in the field of view of the spectrometers. However, the probing with protons using the velocity discrimination method of Post, et al.[12] may be possible using beam probing, if the endothermic reactions prove practical.

1. Laser-Produced Jet

A focused laser beam can be made to produce a rather collimated jet of atoms from a target[20]. The target could either be at the wall, the limiter, or on an inserted wire probe. Through expansion and ionization[21] the lithium density would decay to the level desired in a distance of a few to 10 cms. Such a jet would serve to probe the singly-ionized species in the outer regions in the first case; higher stages of ionization would follow as the physics of the interactions is developed.

2. Pellet Injection

A more sophisticated method that would permit deeper probing into the hot core of the plasma is the injection of small lithium pellets[22],

such as under development by Foster, et al. for refueling with frozen deuterium[23]. The velocities are ~ 10 km/sec, very similar to that of laser vaporization of neutrals described above. At these velocities the lithium donor atoms are essentially stationary (0.07 eV) compared to the plasma ions, so that the Doppler widths of the measured product lines would reflect the temperature of the receptor ions. One would measure in the "tail of the comet" as the density falls and achieve a localized measurement at decreasing densities. Also observed would be the vaporization of the pellet and the effect on the plasma, a matter of great interest in refueling.

In the non-resonance-enhanced model above, one can consider a (p,H) reaction again here giving the local neutral hydrogen (deuterium) density behind the refueling pellet. Then the (H,α) reaction will give the localized α-particle density.

V. SUMMARY

Two types of photon-induced charge transfer processes are discussed from the viewpoint of density diagnostics on plasmas. In the first case (requiring higher laser power density), the electron is transferred to a receptor ion from an excited virtual state in a neutral atom. An attraction here is the possibility of a shifted emission line, affording enhanced contrast to background emission. A combination of (p,H) and (α,H) reactions could be used to measure the α-particle density from the known proton density.

In the second case considered, resonance enhancement of the cross section is achieved by pumping an allowed level in the donor atom from

which charge transfer takes place with a high probability and reduced laser power. Use of resonantly-pumped excited donor atoms permits a direct measurement of the donor state density by resonance fluorescence in the "visible" region with a state-of-the-art dye laser. Numerous examples of resonances involving such typical plasma elements as H, He, Li, C, N, O and Si are given. This is promising for impurity diagnostics near walls and limiters, for example.

It is suggested that the donor atoms be injected either by a laser beam focused on a target near the wall or limiter, or by a traversing pellet[22,23]. The density measured behind the pellet would serve as a local plasma diagnostic (at some distance removed), and could also indicate the effect of the pellet on the plasma during a refueling operation (close to the pellet).

Both of these processes have been proven in other situations and need now to be applied to elements of (fusion) plasma diagnostic interest. The promise of temporally- and spatially-resolved local measurements of density with improved precision and with available apparatus is very attractive in understanding the operation and fueling of potential fusion devices.

REFERENCES

1. S. I. Yakovlenko, Sov. J. Quantum Electron. 8, 151 (1978).

2. D. A. Copeland and C. L. Tang, J. Chem. Phys. 65, 3161 (1976) and 66, 5126 (1977).

3. W. R. Green, M. D. Wright, J. F. Young, and S. E. Harris, Phys. Rev. Lett. 43, 120 (1979).

4. N. Dutta, R. Tkach, D. Frohlich, C. L. Tang, H. Mahr, and P. L. Hartman, Phys. Rev. Lett. 42, 175 (1979).

5. J. D. Power, QCPE Program 233, Quantum Chemistry Program Exchange, Chemistry Department, Indiana University.

6. R. D. Piacentini and A. Salin, J. Phys. B 10, 1515 (1977).

7. W. L. Nutt, R. W. McCullough, K. Brady, M. B. Shah, and H. B. Gilbody, J. Phys. B 11, 1457 (1978).

8. D. R. Bates, R. T. S. Darling, S. C. Hawe, and A. L. Stewart, Proc. Phys. Soc. A (London) 67, 533 (1954).

9. David E. Ramaker and James M. Peek, Atomic Data 5, 167 (1973).

10. T. J. Morgan, J. Geddes, and H. B. Gilbody, J. Phys. B 6, 2118 (1973).

11. J. C. Stewart, J. M. Peek, and J. Cooper, Astrophys. J. 179, 983 (1973).

12. D. E. Post, D. R. Mikkelsen, R. A. Hulse, L. D. Stewart, and J. C. Weisheit, Princeton Plasma Physics Laboratory Report 1592 (1979).

13. W. B. West, E. S. Ensberg, and K. H. Burrell, Paper No. E-17 and private communication (KHB), Third APS Topical Conference on High Temperature Plasma Diagnostics, UCLA, March 17-19, 1980; Bull. Am. Phys. Soc. (to be published).

14. W. L. Fite, A. C. H. Smith, and R. F. Stebbings, Proc. Roy. Soc. (London) A270, 527 (1962).

15. A. Dalgarno, Phil. Trans. Roy. Soc. London A250, 426 (1958).

16. M. R. C. McDowell, Proc. Phys. Soc. (London) A72, 1087 (1958).

17. Atomic and Molecular Processes, D. R. Bates, ed., (Academic Press, New York, 1962).

18. J. B. Hasted, Physics of Atomic Collisions, first edition (Butterworth Press, London, 1964) and second edition (American Elsevier Press, New York, 1972).

19. J. W. Bond, Jr., K. M. Watson, and J. A. Welch, Jr., Atomic Theory of Gas Dynamics, (Addison-Wesley Publishing Co., Reading, MA, 1965).

20. S. A. Cohen, J. L. Cecchi, and E. S. Marmar, Phys. Rev. Lett. 35, 1507 (1975).

21. K. McCormick, "Cross Sections and Rate Coefficients for the Interaction of a Monoenergetic Neutral Lithium Beam with A Maxwellian Plasma", Report No. IPP III/40, January 1978, Max-Planck Institut für Plasmaphysik, Garching bei München, W. Germany.

22. E. S. Marmar, J. L. Cecchi, and S. A. Cohen, Rev. Sci. Instrum. 46, 1149 (1975).

23. C. A. Foster, Paper No. E-2, Third APS Topical Conference on High Temperature Plasma Diagnostics", UCLA, March 17-19, 1980; Bull. Am. Phys. Soc. (to be published).

TABLE 1. Lithium Donors

$$D^* + R^+ \rightarrow R^* + D^+ + \Delta E$$

D	D*	λ_L (Å)	P*	Level	λ (Å)	$\Delta\nu$ (cm^{-1})	ΔE(eV)
Li(2s ^{2}S)	2p ^{2}P	6708	H	2p	(1216)	(-1163)	(-0.14)
			He	2p ^{3}P	10830	647	0.080
			C	3s ^{1}P	2479	256	0.032
			O	3s ^{3}S	(1302)	(4459)	0.55
	3p ^{2}P	3233	H	3d	6562	(-375)	(-0.047)
			He	3p ^{3}P	3889	190	0.024
			C	3d ^{1}D	11330	579	0.072
			O	4s ^{3}S	13164	1050	0.13
			Si	4p ^{1}S	9413	1573	0.20
	4p ^{2}P	2741	H	4d	4861	(-162)	(-0.020)
			He	4p ^{3}P	3188	82	0.010
			C	4d ^{1}D	6828	305	0.038
			O	5s ^{3}S	7254	407	0.050
			Si	5p ^{1}S	5772	418	0.052
	5p ^{2}P	2562	H	5d	4340	(-84)	(-0.010)
			He	5p ^{3}P	2945	44	0.0055
			C	5d ^{1}D	(5771)	164	0.020
			O	6s ^{3}S	6046	200	0.025
			Si	6p ^{1}S	?	?	?
	6p ^{2}P	2475	H	6d	4102	(-45)	(-0.0056)
			He	6p ^{3}P	(2830)	31	0.0038
			C	6d ^{1}D	(5325)	94	0.012
			O	7s ^{3}S	(5556)	117	0.015
			Si	7p ^{1}S	?	?	?
	2s ^{2}S(a)	6708	None				

(a) Obtained for 2p ^{2}P saturated

TABLE 2. Helium Donors

$$D^* + R^+ \rightarrow R^* + D^+ + \Delta E$$

D	D*	λ(Å)	P*	Level	λ(Å)	Δν(cm^{-1})	ΔE(eV)
He(2s ^{3}S)	3p ^{3}P	3889	H	--			
			Li	--			
			C	3d ^{1}D	9406	390	0.048
			O	4s ^{3}S	13164	860	0.11
			Si	4p ^{1}S	9413	1384	0.17
	4p ^{3}P	3188	H	--			
			Li	--			
			C	4d ^{1}D	6828	223	0.028
			O	5s ^{3}S	7254	326	0.040
			Si	5p ^{1}S	5772	336	0.042
	5p ^{3}P	2945	H	--			
			Li	--			
			C	5d ^{1}D	(5771)	120	0.015
			O	6s ^{3}S	6046	156	0.019
			Si	6p ^{1}S	?	?	?
	6p ^{3}P	(2830)	H	--			
			Li	--			
			C	6d ^{1}D	6655	63	0.0078
			O	7s ^{3}S	(5556)	85	0.010
			Si	7p ^{1}S	?	?	?

TABLE 3. Helium Donors ($2\ ^3P \rightarrow n\ ^3S$)

$$D^* + R^+ \rightarrow R^* + D^+ + \Delta E$$

D	D*	λ(Å)	P*	Level	λ(Å)	Δν(cm^{-1})	ΔE(eV)
He($2p\ ^3P$)(a)	$3s\ ^3S$	7065	H	--			
			Li	$3s\ ^2S$	8126	1206	0.14
			C	$3p\ ^1S$	8335	1765	0.22
			O	--			
			Si	--			
	$4s\ ^3S$	4713	H	--			
			Li	$4s\ ^2S$	4972	456	0.057
			C	$4p\ ^1S$	4932	550	0.068
			O	--			
			Si	$4d\ ^1D$	1991	1226	0.15
	$5s\ ^3S$	4121	H	--			
			Li	$5s\ ^2S$	4273	217	0.027
			C	$5p\ ^1S$	4228	226	0.028
			O	$5p\ ^3P$	3692	998	0.12
			Si	$5d\ ^1D$	7680	477	0.059
	$6s\ ^3S$	3869	H	5d	4340	1007	0.12
			Li	$6s\ ^2S$	3986	119	0.015
			C	$6p\ ^1S$	3794	99	0.012
			O	$6p\ ^3P$	3434	544	0.067
			Si	$6d\ ^1D$	6722	210	0.026

(a) Saturated by 1.06 μm laser from $2s\ ^3S$

TABLE 4. Helium Donors ($2\ ^3P \rightarrow n\ ^3D$)

$$D^* + R^+ \longrightarrow R^* + D^+ + \Delta E^1$$

D	D*	λ(Å)	P*	Level	λ(Å)	Δν (cm^{-1})	ΔE(eV)
He($2p\ ^3P$)(a)	$3d\ ^3D$	5876	H	3d	6562	(-28)	(-0.0034)
			Li	$3p\ ^2P$	3233	347	0.043
			C	$3d\ ^1F$	16890	76	0.0094
				$4s\ ^1P$	10541	265	0.033
			O	$3d\ ^3D$	11287	134	0.017
			Si	$3d\ ^1P$	2631	146	0.018
	$4d\ ^3D$	4471	H	4d	4861	(-16)	(-0.0020)
			Li	$4p\ ^2P$	2741	146	0.018
			C	$4d\ ^1P$	8820	1.1	0.00013
				$5s\ ^1P$	8873	71	0.0088
			O	$4d\ ^3D$	7002	57	0.0070
			Si	$4d\ ^1P$	2303	74	0.0091
	$5d\ ^3D$	4026	H	5d	4340	(-11)	(-0.0013)
			Li	$5p\ ^2P$	2562	72	0.0089
			C	$6s\ ^1P$	7241	4.6	0.00057
			O	$5d\ ^3D$	(5960)	29	0.0036
			Si	$5d\ ^1P$	2177	42	0.0052
	$6d\ ^3D$	(3821)	H	6d	4102	(-9)	(-0.0011)
			Li	$6p\ ^2P$	2475	40	0.0050
			C	$6d\ ^1D$	6655	130	0.016
			O	$6d\ ^3P$	(5514)	15	0.0019
			Si	$6d\ ^1P$	(2115)	25	0.0031

(a) Saturated from $2s\ ^3S$

TABLE 5. Hydrogen (or Deuterium)

$$D^* + R^+ \rightarrow R^* + D^+ + \Delta E$$

D	D*	λ(Å)	P*	Level	λ(Å)	Δν(cm^{-1})	ΔE(eV)
H(2p)(a)	3d	6563	He	$3d\ ^3D$	5876	28	0.0035
				$3p\ ^3P$	3889	565	0.070
			Li	$3d\ ^2D$	6104	17	0.0021
				$3p\ ^2P$	3233	375	0.047
			C	$3d\ ^1F$	16890	103	0.013
				$4s\ ^1P$	10541	293	0.036
			O	$3d\ ^3D$	11287	162	0.020
			Si	$3d\ ^1P$	2631	173	0.021
	4d	4861	He	$4d\ ^3D$	4471	17	0.0021
				$4p\ ^3P$	3188	245	0.030
			Li	$4d\ ^2D$	4603	9	0.0011
				$4p\ ^2P$	3233	162	0.020
			C	$4d\ ^1F$	8820	18	0.0022
				$5s\ ^1P$	8873	88	0.011
			O	$4f\ ^3F$	18244	14	0.0017
				$4d\ ^3D$	7002	74	0.0091
			Si	$4d\ ^1P$	2303	91	0.011
H(2p)	5d	4340	He	$5d\ ^3D$	4026	13	0.0016
				$5p\ ^3P$	2945	129	0.016
			Li	$5d\ ^2D$	4133	4	0.00049
				$5p\ ^2P$	2562	83	0.010
			C	$6s\ ^1P$	7241	16	0.0020

(a) Saturated from 1s or 2s

Continued on next page

TABLE 5. Hydrogen (or Deuterium) (Continued)

D	D*	λ(Å)	P*	Level	λ(Å)	Δν (cm^{-1})	ΔE(eV)
H(2p)(a) (Continued)	5d	4340	C	5d ^1D	7365	247	0.031
			O	5f ^3F	12570	7	0.00086
				5d ^3D	(5960)	(40)	(0.0050)
			Si	5d ^1P	2177	53	0.0066
	6d	4102	He	6d ^3D	3821	10	0.0012
				6p ^3P	2830	77	0.0095
			Li	6d ^2D	3915	3	0.00037
				6p ^2P	2475	49	0.0060
			C	6d ^1D	6655	139	0.017
				6p ^1D	3961	555	0.069
			O	6f ^3F	10753	5	0.00062
				6d ^3D	5514	24	0.0030
			Si	6d ^1P	2115	34	0.0042

TABLE 6. Sodium Donors

$$D^* + R^+ \rightarrow R^* + D^+ + \Delta E$$

D	D*	λ(Å)	P*	Level	λ(Å)	Δν (cm^{-1})	ΔE(eV)
Na($3s\ ^2S$)	$3p\ ^2P$	5890	H	2p	(1216)	2934	0.36
			He	$2p\ ^1P$	(20581)	2697	0.33
			Li	--			
			C	$3s\ ^1P$	2479	4353	0.54
			O	--			
			Si	$4s\ ^1P$	3905	270	0.033
	$4p\ ^2P$	3302	H	3d	6503	1007	0.12
			He	$3p\ ^1P$	5016	928	0.12
			Li	--			
			C	$3d\ ^1P$	10124	910	0.11
			O	$3d\ ^3P$	11287	1170	0.15
			Si	$3d\ ^1P$	2631	1182	0.15
	$5p\ ^2P$	2853	H	4d	4861	447	0.055
			He	$4p\ ^1P$	3965	416	0.052
			Li	--			
			C	$4d\ ^1P$	6588	380	0.047
			O	$4d\ ^3P$	7002	521	0.065
			Si	$4d\ ^1P$	2303	538	0.067
	$6p\ ^2P$	2677	H	5d	4340	234	0.029
			He	$5p\ ^1P$	3614	421	0.052
			Li	--			

(a) Obtained when $3p\ ^2P$ is saturated

Continued on next page

TABLE 6. Sodium Donors (Continued)

D	D*	λ(Å)	P*	Level	λ(Å)	Δν (cm⁻1)	ΔE(eV)
Na(3s ^{2}S) (continued)	6p ^{2}P	2677	C	5d ^{1}P	5669	177	0.022
			O	5d ^{3}P	(5960)	276	0.034
			Si	5d ^{1}P	2177	288	0.036
3s ^{2}S(a)	5890		None				

TABLE 7. Aluminum Donors

$$D^* + R^+ \rightarrow R^* + D^+ + \Delta E$$

D	D*	λ(Å)	P*	Level	λ(Å)	Δν (cm^{-1})	ΔE(eV)
Aℓ($3p\ ^2P$)	$4s\ ^2S$	3944,61	H	2p	(1216)	4488	0.56
			He	$2p\ ^1P$	(20581)	4250	0.53
			Li	--			
			C	--			
			O	--			
			Si	$4s\ ^1P$	3905	1824	0.23
	$5s\ ^2S$	2652	H	3d	6563	1597	0.20
			He	$3p\ ^1P$	5016	1518	0.19
			Li	--			
			C	$3d\ ^1P$	10124	1500	0.19
			O	$3d\ ^3D$	11287	1760	0.22
			Si	$3s\ ^1P$	2532	287	0.036
	$6s\ ^2S$	2372	H	4d	4861	721	0.089
			He	$4p\ ^1P$	3965	690	0.086
			Li	--			
			C	$4d\ ^1P$	6588	655	0.081
			O	$4d\ ^3D$	7002	796	0.099
			Si	$4d\ ^1P$	2303	812	0.10
	$7s\ ^2S$	2200	H	5d	4340	381	0.047
			He	$5p\ ^1P$	3614	368	0.046
			Li	--			

Continued on next page

TABLE 7. Aluminum Donors (Continued)

D	D*	λ(Å)	P*	Level	λ(Å)	Δν (cm^{-1})	ΔE(eV)
Aℓ($3p\ ^2P$) Continued	$7s\ ^2S$	2200	C	$5d\ ^1P$	5669	324	0.040
			O	$5d\ ^3P$	(5960)	423	0.052
			Si	$5d\ ^1P$	2177	436	0.054

END

DATE
FILMED

9-80

DTIC